



# Determination of the Critical Micelle Concentration of Neutral and Ionic Surfactants with Fluorometry, Conductometry, and Surface Tension—A Method Comparison

Norman Scholz<sup>1</sup> · Thomas Behnke<sup>1</sup> · Ute Resch-Genger<sup>1</sup>

Received: 31 October 2017 / Accepted: 4 January 2018 / Published online: 13 January 2018  
© Springer Science+Business Media, LLC, part of Springer Nature 2018

## Abstract

Micelles are of increasing importance as versatile carriers for hydrophobic substances and nanoprobe for a wide range of pharmaceutical, diagnostic, medical, and therapeutic applications. A key parameter indicating the formation and stability of micelles is the critical micelle concentration (CMC). In this respect, we determined the CMC of common anionic, cationic, and non-ionic surfactants fluorometrically using different fluorescent probes and fluorescence parameters for signal detection and compared the results with conductometric and surface tension measurements. Based upon these results, requirements, advantages, and pitfalls of each method are discussed. Our study underlines the versatility of fluorometric methods that do not impose specific requirements on surfactants and are especially suited for the quantification of very low CMC values. Conductivity and surface tension measurements yield smaller uncertainties particularly for high CMC values, yet are more time- and substance consuming and not suitable for every surfactant.

**Keywords** Surfactant · CMC · Micelle · Conductometry · Surface Tension · Nile Red · DPH · Pyrene · Fluorescence · Optical probe

## Introduction

Micelles are ordered structures of neutral or ionic amphiphilic surfactant molecules of small size (10–100 nm), which are formed in aqueous solution by self-assembling, driven by attractive interactions between the surfactants' hydrophilic parts and water molecules and minimizing interactions of the surfactant's hydrophobic moieties with water molecules [1–6]. These simply prepared, deformable and biocompatible systems, that are often even biodegradable, are used e.g., as carriers for hydrophobic substances like drugs, catalysts, and sensor molecules in pharmaceutical, diagnostic, medical, and therapeutic applications [1, 5–9]. The key parameter, which characterizes the formation and stability of micelles is the critical micelle concentration (CMC), i.e., the surfactant concentration required for spontaneous

micelle formation [1, 3, 6, 8, 10–12]. Several methods have been meanwhile developed for CMC measurements. This includes reporter-free physicochemical methods like light scattering [13], surface tension [14–18], and electric conductivity [13, 19–21], that utilize changes of macroscopic parameters for CMC determination [6, 20]. CMC values can be also obtained photometrically or fluorometrically with the aid of suitable optical probes, i.e., dyes with polarity- or viscosity-sensitive spectroscopic properties [10, 12, 15, 19, 21–27]. Fluorometric parameters exploited for CMC signaling include changes in the spectral position intensity, ratio and intensity of the probe's emission spectrum. Also changes in its emission anisotropy that arise from changes in the reporter's microenvironment upon micelle formation, can be utilized. All these optical measurements assume that the reporter, which is added in a very low concentration, does not affect micelle formation and the CMC.

Despite the general importance of CMC values and their frequent measurements, there are still considerable inconsistencies in CMC values reported in the literature, even for common surfactants. This is exemplarily summarized in Table 1 for one of the most frequently used cationic surfactants cetyltrimethylammonium bromide

✉ Ute Resch-Genger  
ute.resch@bam.de

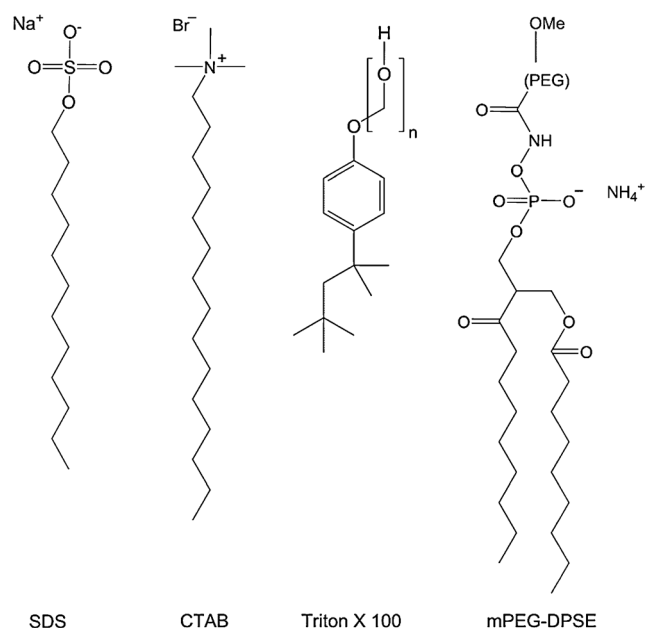
<sup>1</sup> Division Biophotonics, Federal Institute for Materials Research and Testing (BAM), Richard-Willstaetter-Str.11, D-12489 Berlin, Germany

**Table 1** Comparison of representative CMC values of CTAB (given in mM) taken from the literature using different determination methods

Method	Parameter	Reporter	CMC
Fluorescence	Change in band ratios (vibronic fine structure)	Pyrene	0.897 [19]
Fluorescence	Change in band ratios (vibronic fine structure)	Pyrene	0.8 [28]
Fluorescence	Intensity	Coumarin 153	0.83 [12]
Fluorescence	Spectral shift of $I_{\max}$	Coumarin 153	0.86 [12]
Fluorescence	Anisotropy	DPH	0.65 [22]
Surface tension	Surface tension	-	0.96 [14]
Conductivity	Conductivity	-	0.98 [19]

(CTAB). These deviations can arise, e.g., from method-inherent pitfalls, the presence of (unknown) impurities in commercial surfactants originating e.g. from surfactant synthesis, and from the method used for data analysis. Moreover, due to the lack of systematic comparisons of reporter-free and reporter-dependent methods, it cannot be excluded that probe molecules affect the CMC despite the very low reporter concentration required for fluorescence measurements, possibly even in a compound- and surfactant-specific manner. In addition, the CMC is often given only as a concentration range instead of as a surfactant concentration with an assigned uncertainty.

This encouraged us to systematically assess and compare selected reporter-free physicochemical methods, here conductivity and surface tension and different fluorometric methods for the CMC determination of common ionic and neutral surfactants using different procedures of data analysis. In the case of fluorometry, we also assessed three different fluorescent probes which vary in their spectroscopic properties, particularly the spectral region of their absorption and emission, thereby aiming at providing tools also for micelle systems, which are loaded with other absorbing and/or emitting chromophores. Surfactants studied include cationic CTAB, anionic sodium dodecyl sulfate (SDS), and neutral Triton X as well as the phospholipid methoxy polyethylene glycol-1,2-distearoyl-sn-glycero-3-phosphoethanolamine (mPEG-DSPE). The latter presents a model system for surfactants increasingly used for the design of targeted micelles conjugated to, e.g., biomolecules binding to specific cell surface proteins or other biologically relevant structures [8, 29]. The chemical structures of these surfactants are summarized in Fig. 1. Moreover, also possible influences originating from probe molecules or typical additives in surfactants and buffers like salts are briefly addressed [30, 31].

**Fig. 1** Chemical structures of SDS, CTAB, Triton X 100 ( $n=9-10$ ), and mPEG-DSPE

## Materials and Methods

### Materials

SDS (99% and 95%), CTAB (98%, CTAB), 1,6-diphenyl-1,3,5-hexatriene (98%, DPH), and pyrene (99%) were purchased from Sigma–Aldrich Co. (Steinheim, Germany) and Nile Red from Fluka. Spectroscopic grade tetrahydrofuran (THF) was supplied by Merck (Darmstadt, German). Triton X-100 by Appli-Chem (Darmstadt, Germany), and mPEG-DSPE by Nanocs Inc. (New York City, United States), respectively. Ultrapure reagent water was obtained by running demineralized (by ion exchange) water through a Milli-Q® water purification system (Millipore Synthesis A10, Schwalbach, Germany).

### Methods

#### Preparation of Dye Surfactant Solutions

An aqueous solution of the reporter dye was prepared by adding 1  $\mu$ L of the dye dissolved in THF ( $c=10$  mM) to 5 mL water, yielding a dye concentration of 2  $\mu$ M. Surfactant stock solutions of SDS, CTAB, Triton, and mPEG-DSPE with concentrations of 103.8, 41.5, 17.9 and 1.8 mM, respectively, were obtained by dissolving the respective amounts of the surfactants in aqueous dye solutions. The desired surfactant concentrations were adjusted

by mixing dye-saturated stock solutions of the surfactants with an aqueous solution of the reporter dye. The samples were shaken for 30 min and then transferred to a cuvette or to a microplate well for measurements of fluorescence spectra or fluorescence polarization/emission anisotropy.

## Instrumentation

### Spectroscopic Measurements

Fluorescence spectra of pyrene and the emission anisotropy of DPH were obtained with a FSP 920 spectrofluorometer (Edinburgh Instrument Ltd., Livingston UK) equipped with polarizers in the excitation and emission channel (set to magic angle conditions except for measurements of the emission anisotropy  $r$ ) in standard  $0^\circ/90^\circ$  excitation-emission geometry in 1-cm polystyrene (PS) semi-micro cuvettes (Brand GmbH, Wertheim, Germany). The fluorescence spectra of pyrene were recorded using an excitation wavelength of 335 nm, and the fluorescence intensities  $I_1$  and  $I_3$  were measured at 373 and 384 nm, respectively, corresponding to the dye's first and third vibronic emission band.  $r$  of DPH was obtained using an excitation wavelength of 355 nm, an emission wavelength of 429 nm, and different positions of the excitation and emission polarizers.  $r$  was subsequently calculated from the emission intensities recorded for different settings of the excitation and emission polarizer according to Eq. 1 [32].

$$r = \frac{I_{\parallel} - I_{\perp}}{I_{\parallel} + 2I_{\perp}} \quad (1)$$

Fluorescence spectra and integral fluorescence intensities of Nile Red were obtained with a Tecan Infinite M200Pro microplate reader (Tecan Group Ltd., Männedorf, Switzerland) in 96-well UV-Star® microplates (Greiner Bio-one, Frickenhausen, Germany) using an excitation wavelength of 550 nm. These spectra are not spectrally corrected for the wavelength-dependent spectral sensitivity of the instruments' detection channel in contrast to the spectra obtained with the spectrofluorometer [33].

### Conductivity

The electric conductivity was measured with a WTW LF537 conductometer (WTW, Weilheim, Germany) using a Metrohm double Pt-sheet electrode (Metrohm GmbH, Filderstadt, Germany) with a cell constant of  $1305 \mu\text{S cm}^{-1}$ . A surfactant stock solution was added to pure water and the solution was stirred for 1 min prior to the conductivity measurement.

## Surface Tension

A K100MK2 tensiometer (KRÜSS GmbH, Hamburg, Germany) was employed for the determination of the surface tensions by the Wilhelmy plate method. Before each measurement, the Pt-plate was always cleaned and heated to red/orange color with a Bunsen burner. A surfactant stock solution was added to pure water, the solution was stirred for 1 min before the measurement of the surface tension, which was performed over a period of 180 s.

## Results and Discussion

### Intensity Ratio of the Vibronic Emission Bands of Pyrene

The vibronic structure of the emission spectrum of pyrene depends on polarity. The allowed and strong band  $I_3$  at 384 nm shows minimal intensity variations with solvent polarity in contrast to the peak  $I_1$  at 373 nm, originating from a forbidden transition, the intensity of which is strongly polarity-dependent [28, 34]. Hence, changes in the intensity ratio of  $I_1$  and  $I_3$  provide information on changes in the microenvironment of pyrene and can be exploited to determine the CMC of surfactants [28]. In the absence of surfactant, pyrene senses the polar environment of water molecules yielding a  $I_1:I_3$  ratio of around 1.6. When the CMC is reached, the environment of pyrene becomes increasingly less polar as reflected by a decrease of the  $I_1:I_3$  ratio reaching values of 1.2 above the CMC as found for pyrene in an organic solvent like THF. A plot of the  $I_1:I_3$  ratio of pyrene as function of surfactant concentration is shown in Fig. 2

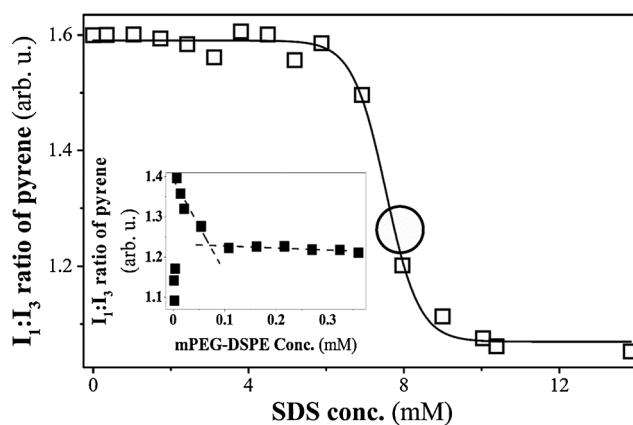


**Fig. 2**  $I_1:I_3$  ratio of pyrene as function of SDS concentration (open squares). The inflection point (black circle) of the Boltzmann fit of the sigmoidal plot of the data (solid line) provides the CMC. Inset:  $I_1:I_3$  ratio as function of mPEG-DSPE concentration (full squares). Here, a reasonable Boltzmann fit of that data is not possible and the CMC can be obtained only from two linear regressions (dashed lines)

exemplarily for SDS. The inflection point of the sigmoidal curve resulting from a Boltzmann fit of the data [1, 5] equals the CMC of SDS [19]. This method is versatile and does not impose requirements on the surfactant like conductivity measurements.

A similar behavior was observed for CTAB and Triton X, while in the case of mPEG-DSPE (see Fig. 2, inset), the  $I_1:I_3$  ratios at low and higher phospholipid concentrations amount to values of about 1.1 and only 1.4, respectively. Above the expected CMC, the  $I_1:I_3$  ratio reaches a constant value of about 1.2. The  $I_1:I_3$  ratios at low phospholipid concentrations are ascribed to the formation of intramolecular micelles, which allows dissolving of small amounts of pyrene in a less polar environment. Such a behavior was also found by Zana and co-workers who compared the  $I_1:I_3$  ratios of the pyrene emission resulting for the determination of the CMC of Triton X and the closely related nonionic surfactant Tyloxapol [35]. For the latter surfactant, formation of intramolecular micelles was observed resulting in a similar behavior of the  $I_1:I_3$  ratios of pyrene as noticed by us for our phospholipid. Hence, for mPEG-DSPE, a sigmoidal fit is not applicable for CMC determination; instead, the CMC was derived from the intersection of two linear fits of the regions of decreasing and constant  $I_1:I_3$  ratios. This approach relying on a two linear regression method was also reported in the literature [1, 5, 36], particularly for studies of amphiphilic polymers.

With the pyrene ratio method, we could obtain uncertainties, i.e., SD values of 1 and 2% for SDS and Triton X. Here, the pyrene molecules are most likely located in the micelle center as suggested by the larger  $I_1:I_3$  ratios [37, 38]. For CTAB and mPEG-DSPE, the corresponding SD values amounted to 29 and 42%, respectively. In the case of CTAB, this is ascribed to interactions of pyrene with the surfactant's quaternary head groups. Also in the case of mPEG-DSPE, interactions of quaternary counter ions and pyrene molecules or the PEG chains can lead to an inhomogeneous microenvironment sensed by different reporter molecules. Moreover, the more polar environment faced by pyrene leads to decreased fluorescence intensities especially at lower surfactant concentrations, also contributing to larger SD values.

### Emission Intensity of a Solvatochromic Reporter Dye

The absorption spectra as well as the emission spectra and the fluorescence quantum yield of solvatochromic reporters like Nile Red are strongly affected by solvent polarity, with an increase in polarity typically resulting in a bathochromic shift in absorption and emission and a reduced fluorescence intensity [39–41]. Hence, measurements of the fluorescence intensity at a single emission wavelength can be utilized for CMC determination. Such measurements are principally more straightforward and versatile than the intensity ratio

method, that relies solely on the reporter pyrene with its short wavelength absorption and emission prone to interferences from background absorption, autofluorescence originating from impurities often present in surfactants, and scattering. Principally, a broad variety of charge transfer (CT) operated fluorophores can be used, which enables the choice of an optimum wavelength region regarding sensitivity and prevention of undesired signal contribution; this can be particularly advantageous for systems which contain already a chromophore. We chose here Nile Red absorbing and emitting in the visible and red wavelength region as follows from Fig. 3, summarizing the absorption (left) and emission (right) spectra of this dye representatively in water–Triton X mixtures of increasing surfactant concentration (0.2–0.9 mM). As follows from this figure, in water, where this dye is barely soluble, Nile Red reveals a broadened absorption band suggesting the formation of dye aggregates; and is non or barely emissive [42]. An increasing surfactant concentration results in the appearance of an increasingly intense broad emission; this fluorescence enhancement is attributed to the dissolution of (non-emissive) dye aggregates formed in the aqueous phase and solubilization of Nile Red molecules in the considerably less polar micelle core [7, 12, 25, 42]. The long wavelength emission together with the negligible fluorescence in water and the strong fluorescence enhancement upon micelle formation are ideal prerequisites for high sensitivities and low detection limits. A possible pitfall of this method presents the fact that measurements of fluorescence intensities at a single emission wavelength can be generally affected by fluctuations of the excitation light intensity, whereas in the case of all ratiometric measurements like the pyrene method or measurements of the

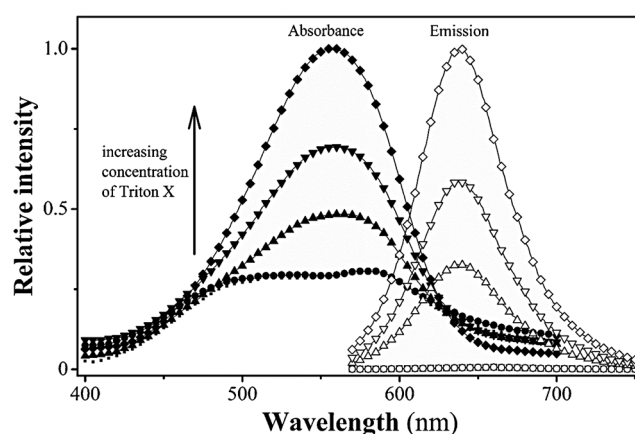


**Fig. 3** Absorption (solid symbols) and emission (hollow symbols) spectra of Nile Red ( $c = 2 \times 10^{-6}$  M) in Triton X solution ( $c = 0.03$ , 0.13, 0.74, 1.12, and 1.60 mM). Broad absorption bands are indicators for aggregates of Nile Red. Above the CMC, the emission intensity of Nile Red increases strongly

emission anisotropy, such fluctuations are cancelled out. Such fluctuations are typically only in the order of maximum 10%.

With this method, the CMC can be subsequently derived from the fluorescence intensity of Nile Red at 648 nm as function of the surfactant concentration. This is exemplarily shown for SDS and Triton X in Fig. 4. In the case of SDS as well as CTAB (data not shown), which bear both hydrophobic chains of uniform length, this yields sigmoidal curves and the CMC can be determined from the inflection point using a Boltzmann fit [7]. This gave SD values of the CMC determination of 3% for CTAB and SDS, respectively.

A different behavior was observed for Triton X and mPEG-DSPE. Here, a clearly detectable emission is observed already at relatively low surfactant concentrations followed by a steadily increasing emission intensity of the reporter dye at higher surfactant concentrations without reaching a plateau. These two surfactants consist both of molecules of varying length of the polyethylene units, which can possibly favor the formation of premicellar aggregates below the CMC, accounting for the observed effects [12]. In this case, the CMC can be obtained from the intersection of two linear fits of the two different fluorescence intensity regions, i.e., the low intensity region at very low surfactant concentration and the region with steadily increasing emission. This fitting procedure leads to slightly higher uncertainties of the CMC of Triton X and mPEG-DSPE with SD values of 13% and 11%, respectively. Our CMC values are in a good agreement with the data obtained in other fluorometric CMC studies using e.g., 8-anilino-1-naphthalenesulfonic acid [10], rhodamine 6G [10], coumarin 480 (Triton X) [10], coumarin 153 (Triton X, SDS, CTAB) [12], and DPH (Triton X, SDS) [25] as fluorescent reporters.

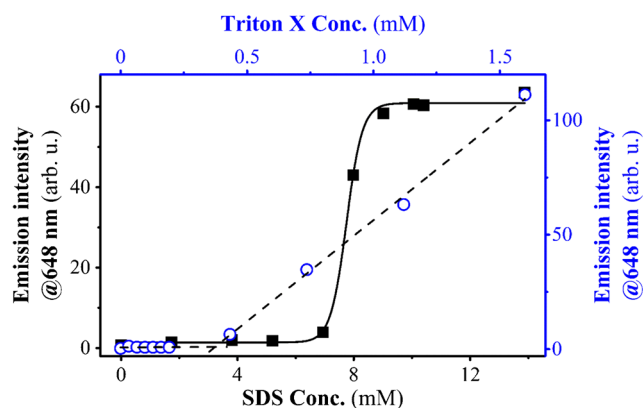


**Fig. 4** Emission intensity of Nile Red at 648 nm in SDS (squares) and Triton X (open blue circles) solutions. The inflection point of a Boltzmann fit of the resulting sigmoidal curve (black line) provides the CMC of SDS. The CMC for Triton X can be derived from the intersections of two linear fits (black dotted lines)

## Changes in Fluorescence Anisotropy

This method relies on a fluorophore, the emission anisotropy of which undergoes considerable changes upon micelle formation. Although measurements of  $r$  are more tedious and less sensitive compared to simple fluorescence intensity measurements at a single excitation and emission wavelength, such measurements are independent of fluctuations of the excitation light intensity. Also, emission anisotropies are independent of dye concentration [7, 12, 25]. The determination of  $r$  can be challenging for low emission intensities, i.e., at low surfactant concentrations, resulting in rather large SD values. There are several reports on this method utilizing reporter dyes, which are excitable at different excitation wavelengths and emit in different wavelength regions. For example, Chaudhuri et al. [22] compared the suitability of the probes 7-hydroxy flavone, 1-pyrene carboxaldehyde, and phenosafranine for the determination of the CMC of SDS, CTAB, and Triton X, using sharp changes in  $r$  as criterion for the CMC. Interestingly, none of the probes were found to be suitable for all surfactants. This was ascribed to Coulombic interactions, photodegradation, and very small changes of  $r$  below and above the CMC [22]. Nevertheless, there are also reports on sigmoidal anisotropy plots, e.g., for curcumin and SDS, CTAB, and Tween derivatives [7]. Disadvantageous of this otherwise interesting dye is, however, its capability to coordinate cations, preventing CMC measurements of cationic surfactants.

For our method comparison, we chose DPH, which forms aggregates in aqueous environments, resulting in a relatively high  $r > 0.1$  and a reduced fluorescence. In an organic solvent like THF, however, DPH reveals  $r$  of 0.04 [7, 22, 25]. Solubilization of the DPH molecules in the micelle cores above the CMC leads continuously to a decrease of  $r$  until a constant plateau is reached [25]. During the measurements of the emission spectra of DPH in the wavelength region of 370 to 600 nm, we noticed, however, a significant loss of the initial fluorescence intensity by up to 80% within 10 min in the presence of our surfactants, particularly for SDS. Interestingly, a solution of DPH in THF measured under the same conditions did not show any loss in fluorescence. The observed emission reduction is attributed to DPH photodecomposition, which is obviously favored by surfactants. Such photoinstabilities were also described in the literature [43]. In order to overcome this limitation, we performed intensity measurements at a single emission wavelength of 429 nm to minimize light exposure of DPH. The results of a typical  $r$  measurement with DPH are shown in Fig. 5 exemplarily for Triton X. Here two regions can be distinguished. While the region below the CMC is characterized by a higher  $r$  and large SD values originating from the very low emission intensities,  $r$  decreases with increasing surfactant concentration and becomes constant independent

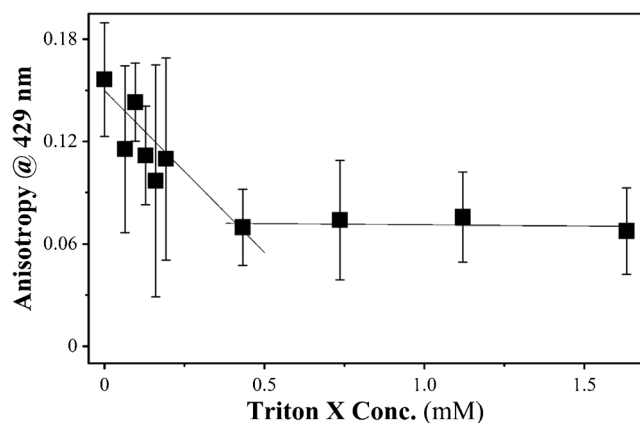


**Fig. 5** Decrease of the fluorescence anisotropy of DPH (measured at 429 nm) with increasing Triton X concentration and corresponding linear fits (black lines), with intersection point equaling the CMC. The error bars represent SD values from at least seven measurements

of surfactant concentration above the CMC. It should be noted, that opposed to free reporter dyes, covalently bound reporter molecules show an increasing anisotropy after micelle formation.

The CMC can be derived here from the intersection point of two linear fits as shown in Fig. 5 exemplarily for Triton X, yielding a CMC of  $0.33 \pm 0.1$  mM for this surfactant. The results of our CMC measurements of SDS and Triton X are in good agreement with CMC values reported by Zhang et al. [25], yet the SD values are about 30%.

### Conductivity Measurements

Conductivity measurements, that do not require expensive instrumentation and a reporter, can be applied exclusively for charged, i.e., ionic surfactants, because non-ionic surfactant molecules do not contribute or change the electric conductivity of a solution. An example for a conductometric CMC measurement is shown in Fig. 6 for CTAB.

As follows from this figure, initially, the conductivity increased linearly upon addition of CTAB due to the increased amount of dissolved anions ( $\text{Br}^-$ ) and cations (cetyltrimethylammonium ions,  $\text{CTA}^+$ ). Above the CMC, CTAB micelles are formed from  $\text{CTA}^+$  cations, with the  $\text{Br}^-$  counter anions being located close to the micelle surface. Further addition of CTAB leads to a less pronounced, yet still linear increase in conductivity, resulting in a smaller slope (see Fig. 6) as in the concentration range above the CMC, with the conductivity mainly arising from  $\text{Br}^-$  counter anions [44]. A similar behavior is observed for the anionic surfactant SDS. mPEG-DSPE, however, reveals a clearly different behavior as highlighted in Fig. 7. Here, generally smaller changes in conductivity and a more or less linear increase of this quantity with increasing surfactant

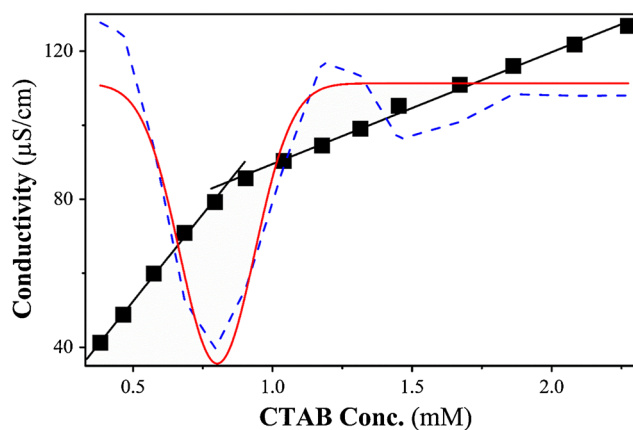


**Fig. 6** Change of conductivity with increasing CTAB concentration (black squares) and corresponding linear fits (black lines), with the intersection point equaling the CMC (Williams method). The CMC can be alternatively obtained from the 2nd derivative of the plot (blue dotted line) and the corresponding Gaussian fit (red line), with the minimum of this fit providing the CMC (Phillips method)

concentration over the whole concentration range of mPEG-DSPE addition are noticed. This is ascribed to the reduced mobility of the ions in mPEG-DSPE.

Two different methods of data analysis can be used to calculate the CMC from such conductivity plots, the Williams method [20, 45, 46] and the Phillips (classical) method [20, 45, 47]. The former determines the CMC from the intersection point of two linear fits of the surfactant concentration range below and above the CMC (solid black line in Fig. 6) and the latter from the 2nd derivative of the plot of the surfactant concentration dependence of the conductivity (blue dotted line), with the minimum of the presented Gaussian fit (red) equaling the CMC. The Williams approach is

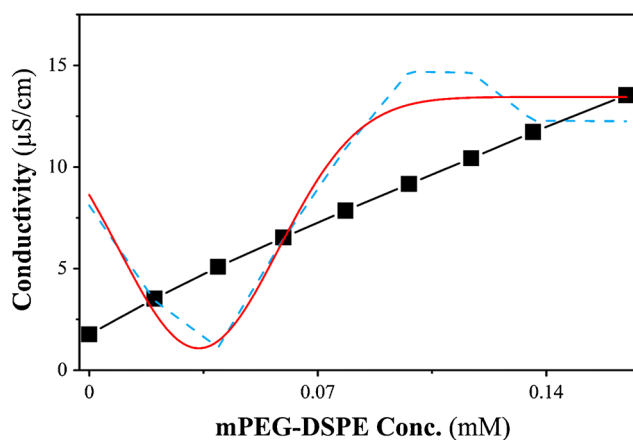


**Fig. 7** Adjusted section change of conductivity with increasing mPEG-DSPE concentration (black squares), the second derivative (blue dotted line), and the corresponding Gaussian fit (red line). The error bars represent SD values derived from three measurements

**Table 2** Comparison of the CMC values (in mM) of CTAB and SDS, obtained from data analysis by the Williams and the Phillips method, respectively

Surfactant	Williams method	Lit.	Phillips method	Lit.
SDS	$8.5 \pm 0.2$	8.28 [20]	$8.5 \pm 0.1$	8.21 [20]
CTAB	$0.80 \pm 0.02$	0.98 [19]	$0.80 \pm 0.01$	$0.92 \pm 0.26$ [45]
mPEG-DSPE	$0.3 \pm 0.1$		$0.04 \pm 0.01$	

applicable for surfactants like CTAB and SDS, which provide strong changes in conductivity and exhibit well distinguishable linear correlations between the measured conductivity and the surfactant concentration and hence, yield linear fits with well distinguishable slopes below and above the CMC.

The Phillips method, which is generally more accurate but more time consuming, is well suited for surfactants like mPEG-DSPE with less or barely discriminable concentration ranges of the measured conductivity and small changes in conductivity (see Fig. 7). The results from the analysis of the conductivity measurements of CTAB, SDS, and mPEG-DSPE with both methods are summarized in Table 2, showing a large deviation for both methods in the case mPEG-DSPE.

## Surface Tension Measurements

The CMC of a surfactant can be obtained also from measurements of the surface tension as function of increasing surfactant concentration [14, 36, 48, 49]. Below the CMC, the surface tension of water decreases with increasing surfactant concentration until the CMC is reached. At this point, the surface tension reaches a minimum or even a constant value indicating the onset of micelle formation. In the literature, there are contradictory reports concerning the shape of the surfactant concentration dependence of the surface tension. Also, different methods of data analysis have been reported. According to Chiu et al. [14], the CMC equals a minimum in the surfactant concentration dependence of the surface tension as demonstrated for CTAB. Patist et al. [16] and Khamis et al. [15], who used this method for the measurement of the CMC of Triton X, did not observe such a minimum, yet two regions differing in the concentration dependence of the surface tension. In these cases, the CMC was derived from the intersection point of two linear fits with different slopes. The results from our measurements are summarized in Fig. 8 exemplarily for CTAB and mPEG-DSPE.

As follows from this figure, in the case of CTAB as well as SDS (data not shown), we clearly observed a minimum in the concentration dependence of the surface tension. Subsequently, we used both methods of data analysis for the calculation of the CMC from our surface tension measurements. The CMC values resulting for CTAB and SDS are summarized in Table 3.

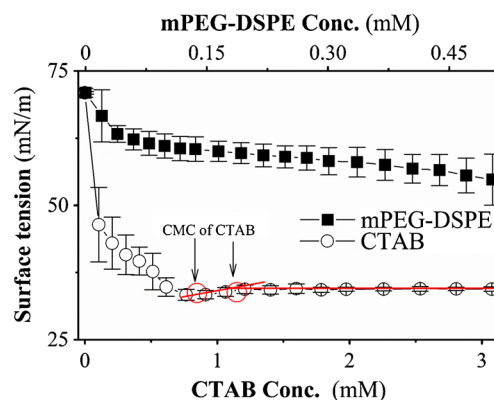


**Fig. 8** Change in surface tension with increasing CTAB (open circles) and mPEG-DSPE concentration (black squares). The CMC equals the intersection point of two linear fits (red lines) according to Khamis et al. [15] and Patist et al. [16] or the minimum (red circle) of the surface tension according to Chiu et al. [14]. The error bars represent SD values derived from three measurements. The black lines are only guides to the eye

**Table 3** CMC values (in mM) of CTAB and SDS determined by surface tension measurements using two different methods of data analysis in comparison to published CMC values determined with the same method

Procedure	CTAB	Lit.	SDS	Lit.
Chiu et al.	$0.8 \pm 0.1$	0.96 [14]	$6.7 \pm 0.35$	10.4 [14]
Khamis et al.	$1.2 \pm 0.02$	0.1 [15]	$8.8 \pm 0.2$	0.8 [15]

Our results agree very well with the data reported by Chiu et al., but exceed the values given by Khamis et al. by a factor of about 10 [14, 15]. The SD values derived by us for CTAB and SDS were 2% (see Table 3). A determination of the CMC of mPEG-DSPE was not possible because neither an intersection point nor a constant region was observed although the mPEG-DSPE concentration was increased by up to a 10-fold excess of the expected CMC although the surface tension method is usually described as generally applicable. We did not attempt to determine the CMC of Triton X with this method as first studies revealed similar effects as observed for mPEG-DSPE. Moreover, surface tension measurements require a larger volume and hence more substance compared to the previously introduced methods for CMC determination. In addition, they are particularly prone to interferences from impurities [15, 16, 48, 49] like conductivity measurements.

## Pitfalls

### Impurities and Salts

CMC measurements can be particularly affected by the ionic strength of added salts and impurities remaining from surfactant synthesis, which can vary amongst suppliers, due to the use of different preparation and purification procedures, from batch to batch. Moreover, in the case of hydroscopic surfactants like mPEG-DSPE, water adsorption can play a role, affecting weighting and hence, precise adjustment of the surfactant concentration. Also, the fluorescent reporter itself, which is often a hydrophobic molecule, and the addition of small amounts of organic solvents like THF typically required for dye solubilization can affect CMC data. Hence, we exemplarily studied the influence of (i) typical reporter or probe molecules and organic solvents, (ii) ionic strength, i.e., here by varying the NaCl, concentration, and surfactant purity on CMC values obtained with different methods. The goal was here to solely screen factors possibly influencing CMC measurement.

### Influence of Fluorescent Probes and Organic Solvents

We representatively measured the CMC of CTAB conductometrically in the presence of two organic dyes, here neutral Nile Red and water soluble cationic Rhodamine 6G, applying fluorophore concentrations of up to 2  $\mu\text{M}$ . Moreover, conductometric measurements were performed without THF and in the presence of 4.0 and 8.0  $\mu\text{M}$  THF, respectively. In all cases, no effects were observable.

### Ionic Strength

In order to assess the influence of this factor, CMC determinations were performed with selected samples of ionic and nonionic surfactants in the presence of 0.9 wt-% NaCl (corresponding to the concentration of an isotonic saline solution), using fluorometry and the neutral reporters pyrene and Nile Red as well as conductometry. As representatively illustrated in Fig. 9 for the pyrene method, the CMC of neutral Triton X is not influenced by NaCl. For cationic CTAB, however, an increase in ionic strength leads to higher aggregation numbers and hence, to a considerably smaller CMC value reduced by a factor of about 10 (Fig. 9). This was also verified by the Nile Red method (see Table 4).

As to be expected, conductivity measurements are considerably affected by ionic strength, with an increase in ionic strength leading to an initially high conductivity of about 10 mS/cm for the isotonic solutions studied here.

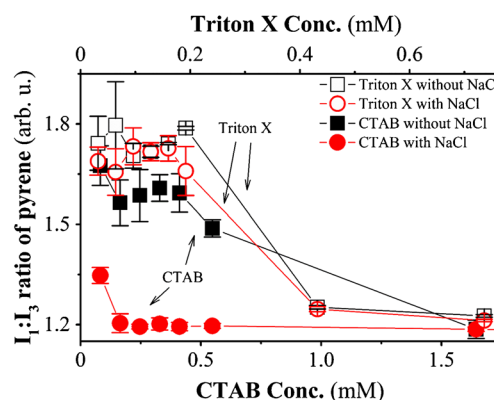


**Fig. 9** Plot of the  $I_1:I_3$  ratios of pyrene as function of the concentration of Triton X (open symbols) and CTAB (solid symbols) without NaCl (black lines) and after addition of 0.9 wt%, NaCl (red lines). The lines connecting the data points are only guides to the eye. The error bars represent the SD of three measurements

**Table 4** Comparison of CMC values (in mM) determined for CTAB, SDS, and Triton X with 0.9 wt%, NaCl and corresponding CMC without NaCl (in brackets)

	Pyrene	Nile Red	Conductivity
SDS 95%	0.7 (3.7)	1.0 (4.6)	--- (4.3)
CTAB	0.08 (0.7)	0.2 (1.2)	--- (0.8)
Triton X	0.3 (0.4)	0.3 (0.3)	Not measurable

Moreover, higher ionic strengths also increase significantly the SD of the measurements as the resulting conductivity values exceed considerably the small changes in conductivity due to micelle formation, thereby interfering with CMC determination or rendering it even impossible. For samples with higher ionic strength, spectroscopic methods should be applied for CMC determination.

### Surfactant Purity

In order to underline the influence of surfactant purity on resulting CMC values, we exemplarily determined the CMC of SDS purchased from two manufacturers or suppliers, with purities of 95 and 99%, reported based upon the total alkyl sulfate content, using all methods assessed in this study. The identification of the chemical nature of these impurities, which are most likely in the majority unreacted educts, i.e., alkyl sulfates, was beyond the scope of our studies. As follows from Fig. 10, the CMC values obtained for less pure SDS amounted always only to half the value obtained for the more pure SDS. This underlines the critical influence of surfactant purity on CMC data.

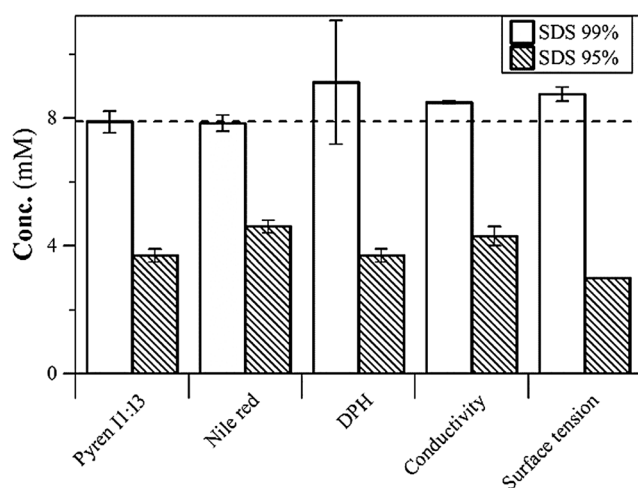


**Fig. 10** CMC values determined for SDS from two different batches with reported purities of 95 and 99%, applying different methods and hence detection principles. The error bars represent the SD of at least three measurements

## Method Comparison

Based upon the results of our measurements, we derived a method comparison summarized in Table 5.

In general, optical methods like fluorescence measurements are very versatile and do not impose specific requirements on the surfactant like charge and enable fast measurements with the sample preparation being usually the most time-consuming step. Crucial for the accuracy can be the choice of the reporter or probe, which must reveal distinct changes of its spectroscopic properties like the spectral shape of its emission spectrum, fluorescence quantum

yield/intensity, or emission anisotropy below and above the CMC. Particularly fluorophores with a low photostability or small changes in the measured spectroscopic quantity accompanying micelle formation should be avoided as this typically results in increased measurement uncertainties. Due to their high sensitivity, fluorometric methods are particularly favorable for the detection of small CMC values below 0.1 mM. These methods require, however, a fluorescence spectrometer, which is typically more expensive than a conductometer or a tensiometer, and in the case of the DPH method, also additional accessories like polarizers. Advantageous of optical measurements can be also the possibility to perform such studies with a microplate reader, which enables a high sample throughput and automated measurements. If CMC measurements are to be done in the presence of encapsulated compounds that are colored or fluorescent, spectral interferences and crosstalk have to be considered for the choice of the reporter dye and type of spectroscopic measurement. Especially favorable is the Nile Red method, due to the high sensitivity provided by this highly emissive dye and its strong changes in fluorescence quantum yield upon micelle formation in combination with a simpler method of data analysis as mandatory for the other two spectroscopic methods. Moreover, this method yields a particularly good reproducibility and precision for all types of surfactants (see also Table 6).

Conductivity and surface tension measurements are reporter free and therefore require less sample preparation steps and need only simple and inexpensive instrumentation. In the case of some surfactants, they can yield relatively small SD values of about 1%, e.g., for SDS. Disadvantages present the larger sample volumes and long measurements times compared to optical-spectroscopic

**Table 5** Advantages and limitations of the methods evaluated for the determination of the CMC of differently charged surfactants

	Spectral change / Pyrene	Intensity / Nile Red	Anisotropy / DPH	Conductivity	Surface tension
Advantages	- Fast measurement - No requirements on samples	- Fast measurement - No requirements on samples - Direct Yes/No decision on micelle formation	- Fast measurement - No requirements on samples	- Reporter free - Ease of sample preparation, i.e., simple titration - Low cost	- Reporter free - Ease of preparation - No requirements on samples
Limitations	- Requires reporter dye - Inaccurate results at low surfactant concentrations - Elaborate sample preparation	- Requires reporter dye - Elaborate sample preparation	- Requires reporter dye - Fast bleaching of DPH - Polarizers needed - Inaccurate results at low surfactant concentrations - Elaborate sample preparation	- Only for charged surfactants - Large sample volume - Long measurement time	- Very large sample volume - Long measurement time
Uncertainties	- Results and uncertainties are surfactant-specific - SD of 142%	- High accuracy / low coefficient of variation - SD of 313%	- Relatively large SD - SD of 530%	- Results and uncertainties depend on data analysis procedure - SD of 117%	- Results and uncertainties depend on data analysis procedure - SD of 212%

**Table 6** CMC values (in mM) for SDS, CTAB, Triton X 100, and mPEG-DSPE as obtained from our studies compared with literature values

Surfactant	Pyrene	Nile Red	DPH	Conductivity	Surface tension	Lit.
SDS	7.9 ± 0.4	7.8 ± 0.3	9.12 ± 1.94	8.5 ± 0.1	6.7 ± 0.4 <sup>a</sup>	7.9 ± 1.5 [11, 12, 14, 15, 17, 19–21, 23–25, 28, 30, 43, 50–52]
CTAB	0.7 ± 0.2	1.2 ± 0.1	0.70 ± 0.41	0.8 ± 0.1	0.8 ± 0.1 <sup>a</sup>	0.9 ± 0.08 [12–15, 19, 28, 30, 50]
Triton X	0.37 ± 0.09	0.30 ± 0.07	0.33 ± 0.13	–	–	0.2 ± 0.06 [10, 11, 15, 16, 19, 23–25, 28, 30, 43]
mPEG-DSPE	0.11 ± 0.05	0.07 ± 0.01	0.15 ± 0.06	0.04 ± 0.01	– <sup>b</sup>	0.02 ± 0.01 [23]

<sup>a</sup> values obtained from the minima surface tension method

<sup>b</sup> Determination from surface tension measurements was not possible

methods. Due to their lower sensitivity, both methods are better suited for the measurement of CMC values above 0.1 mM.

Our study also reveals that CMC determinations and their uncertainties depend on the surfactants itself, e.g., structural properties such as small size-distribution of the hydrophobic chains. For example, surfactants consisting of polymeric moieties or functional groups, which can interact with signal generating reporters, can increase measurement uncertainties significantly (see Figs. 7 and 8). Moreover, also the applied method of data analysis needs to be carefully chosen.

## Conclusion

In summary, we assessed three optical methods, each relying on a different fluorometric quantity, as well as conductivity and surface tension measurements for the determination of the critical micelle concentration (CMC) of four ionic and nonionic surfactants and compared our results to literature data. Our results, summarized in Table 6, underline the advantages of spectroscopic measurements, which can be performed with all types of surfactants and are especially suitable to determine small CMC below 0.1 mM. Our study also suggests that deviations in published data can arise from different sample preparations or compositions, measuring conditions or data evaluation approaches, often in line with insufficient information supplied. This includes e.g., the purity of the surfactants and other chemicals used. In the case of methods relying on reporters and requiring the use of other additives like organic solvents, only low concentrations and small amounts should be applied. If this cannot be avoided control experiments have to be conducted to assure that these compounds do not affect resulting CMC values. Particularly challenging seems to be the CMC determination of PEG derivatives like PLGA-PEG-PLGA triblock copolymer, which can be ascribed to their size/length/molar mass distribution. Here, also spectroscopic methods seem to be better suited than measurements of conductivity and surface tension.

**Acknowledgements** We gratefully acknowledge the financial support from the Federal Ministry for Economic Affairs and Energy (Grant BMWi-10/12) and from the Ph.D. program of BAM. We are grateful to Mrs. G. Hidde for performing the surface tension measurements.

## References

1. Ashjari M, Khoei S, Mahdavian AR, Rahmatolahzadeh R (2012) Self-assembled nanomicelles using PLGA-PEG amphiphilic block copolymer for insulin delivery: a physicochemical investigation and determination of CMC values. *J Mater Sci Mater Med* 23(4):943–953. <https://doi.org/10.1007/s10856-012-4562-1>
2. Faustino CM, Calado AR, Garcia-Rio L (2009) New urea-based surfactants derived from alpha,omega-amino acids. *J Phys Chem B* 113(4):977–982. <https://doi.org/10.1021/jp807396k>
3. Garcia ME, Sanz-Medel A (1986) Dye-surfactant interactions: a review. *Talanta* 33(3):255–264. [https://doi.org/10.1016/0039-9140\(86\)80060-1](https://doi.org/10.1016/0039-9140(86)80060-1)
4. Khan AM, Shah SS (2008) Determination of critical micelle concentration (Cmc) of sodium dodecyl sulfate (SDS) and the effect of low concentration of pyrene on its Cmc using ORIGIN software. *J Chem Soc Pak* 30(2):186–191
5. Song Z, Feng R, Sun M, Guo C, Gao Y, Li L, Zhai G (2011) Curcumin-loaded PLGA-PEG-PLGA triblock copolymeric micelles: preparation, pharmacokinetics and distribution in vivo. *J Colloid Interface Sci* 354(1):116–123. <https://doi.org/10.1016/j.jcis.2010.10.024>
6. Tadros TF (2005) Applied surfactants: principles and applications. Blackwell Science Publ, Oxford. <https://doi.org/10.1002/3527604812>
7. Mondal S, Ghosh S (2012) Role of curcumin on the determination of the critical micellar concentration by absorbance, fluorescence and fluorescence anisotropy techniques. *J Photochem Photobiol B* 115(0):9–15. <https://doi.org/10.1016/j.jphotobiol.2012.06.004>
8. Owen SC, Chan DPY, Shoichet MS (2012) Polymeric micelle stability. *Nano Today* 7(1):53–65. <https://doi.org/10.1016/j.nantod.2012.01.002>
9. Zhu Q, Huang L, Su J, Liu S (2014) A sensitive and visible fluorescence-turn-on probe for the CMC determination of ionic surfactants. *Chem Commun* 50(9):1107–1109. <https://doi.org/10.1039/c3cc45244a>
10. Anand U, Jash C, Mukherjee S (2011) Spectroscopic determination of critical micelle concentration in aqueous and non-aqueous media using a non-invasive method. *J Colloid Interface Sci* 364(2):400–406. <https://doi.org/10.1016/j.jcis.2011.08.047>
11. Nakahara Y, Kida T, Nakatsuji Y, Akashi M (2005) New fluorescence method for the determination of the critical micelle concentration by photosensitive monoazacryptand derivatives. *Langmuir* 21(15):6688–6695. <https://doi.org/10.1021/la050206j>

12. Prazeres TJJ, Beija M, Fernandes FV, Marcelino PGA, Farinha JPS, Martinho JMG (2012) Determination of the critical micelle concentration of surfactants and amphiphilic block copolymers using coumarin 153. *Inorg Chim Acta* 381(0):181–187. <https://doi.org/10.1016/j.ica.2011.09.013>
13. Ghosh S, Krishnan A, Das PK, Ramakrishnan S (2003) Determination of critical micelle concentration by hyper-rayleigh scattering. *J Am Chem Soc* 125(6):1602–1606. <https://doi.org/10.1021/ja029070r>
14. Chiu YC, Kuo CY, Wang CW (2000) Using electrophoresis to determine zeta potential of micelles and critical micelle concentration. *J Dispers Sci Technol* 21(3):327–343. <https://doi.org/10.1080/01932690008913270>
15. Khamis M, Bulos B, Jumean F, Manassra A, Dakiky M (2005) Azo dyes interactions with surfactants. Determination of the critical micelle concentration from acid-base equilibrium. *Dyes Pigments* 66(3):179–183. <https://doi.org/10.1016/j.dyepig.2004.09.012>
16. Patist A, Bhagwat SS, Penfield KW, Aikens P, Shah DO (2000) On the measurement of critical micelle concentrations of pure and technical-grade nonionic surfactants. *J Surfactant Deterg* 3(1):53–58. <https://doi.org/10.1007/s11743-000-0113-4>
17. Staples E, Thompson L, Tucker I, Penfold J, Thomas RK, Lu JR (1993) Surface-composition of mixed surfactant monolayers at concentrations well in excess of the critical micelle concentration - a neutron-scattering study. *Langmuir* 9(7):1651–1656. <https://doi.org/10.1021/La00031a009>
18. Al-Soufi W, Pineiro L, Novo M (2012) A model for monomer and micellar concentrations in surfactant solutions: application to conductivity, NMR, diffusion, and surface tension data. *J Colloid Interface Sci* 370(1):102–110. <https://doi.org/10.1016/j.jcis.2011.12.037>
19. Aguiar J, Carpena P, Molina-Bolivar JA, Ruiz CC (2003) On the determination of the critical micelle concentration by the pyrene 1: 3 ratio method. *J Colloid Interface Sci* 258(1):116–122. [https://doi.org/10.1016/S0021-9797\(02\)00082-6](https://doi.org/10.1016/S0021-9797(02)00082-6)
20. Pérez-Rodríguez M, Prieto G, Rega C, Varela LM, Sarmiento F, Mosquera V (1998) A comparative study of the determination of the critical micelle concentration by conductivity and dielectric constant measurements. *Langmuir* 14(16):4422–4426. <https://doi.org/10.1021/La980296a>
21. Romani AP, Machado AE, Hioka N, Severino D, Baptista MS, Codognoto L, Rodrigues MR, de Oliveira HP (2009) Spectrofluorimetric determination of second critical micellar concentration of SDS and SDS/Brij 30 systems. *J Fluoresc* 19(2):327–332. <https://doi.org/10.1007/s10895-008-0420-4>
22. Chaudhuri R, Guharay J, Sengupta PK (1996) Fluorescence polarization anisotropy as a novel tool for the determination of critical micellar concentrations. *J Photochem Photobiol A* 101(2–3):241–244. [https://doi.org/10.1016/S1010-6030\(96\)04412-7](https://doi.org/10.1016/S1010-6030(96)04412-7)
23. Prieve A, Zalipsky S, Cohen R, Barenholz Y (2002) Determination of critical micelle concentration of lipopolymers and other amphiphiles: comparison of sound velocity and fluorescent measurements. *Langmuir* 18(3):612–617. <https://doi.org/10.1021/La0110085>
24. Wong JE, Duchscherer TM, Pietraru G, Cramb DT (1999) Novel fluorescence spectral deconvolution method for determination of critical micelle concentrations using the fluorescence probe PRODAN. *Langmuir* 15(19):6181–6186. <https://doi.org/10.1021/La981716z>
25. Zhang X, Jackson JK, Burt HM (1996) Determination of surfactant critical micelle concentration by a novel fluorescence depolarization technique. *J Biochem Biophys Methods* 31(3–4):145–150. [https://doi.org/10.1016/0165-022X\(95\)00032-M](https://doi.org/10.1016/0165-022X(95)00032-M)
26. Jumpertz T, Tschapek B, Infed N, Smits SH, Ernst R, Schmitt L (2011) High-throughput evaluation of the critical micelle concentration of detergents. *Anal Biochem* 408(1):64–70. <https://doi.org/10.1016/j.ab.2010.09.011>
27. Cai XT, Yang WJ, Huang L, Zhu QH, Liu SW (2015) A series of sensitive and visible fluorescence-turn-on probes for CMC of ionic surfactants: design, synthesis, structure influence on CMC and sensitivity, and fast detection via a plate reader and a UV light. *Sensors Actuators B Chem* 219:251–260. <https://doi.org/10.1016/j.snb.2015.04.126>
28. Kalyanasundaram K, Thomas JK (1977) Environmental effects on vibronic band intensities in pyrene monomer fluorescence and their application in studies of micellar systems. *J Am Chem Soc* 99(7):2039–2044. <https://doi.org/10.1021/Ja00449a004>
29. Chan DP, Owen SC, Shoichet MS (2013) Double click: dual functionalized polymeric micelles with antibodies and peptides. *Bioconjug Chem* 24(1):105–113. <https://doi.org/10.1021/bc300511a>
30. Cai L, Gochin M, Liu K (2011) A facile surfactant critical micelle concentration determination. *Chem Commun* 47(19):5527–5529. <https://doi.org/10.1039/c1cc10605h>
31. Chattopadhyay A, Harikumar KG (1996) Dependence of critical micelle concentration of a zwitterionic detergent on ionic strength: implications in receptor solubilization. *FEBS Lett* 391(1–2):199–202. [https://doi.org/10.1016/0014-5793\(96\)00733-8](https://doi.org/10.1016/0014-5793(96)00733-8)
32. Lakowicz JR (2006) Principles of fluorescence spectroscopy 3. Auflage edn. Springer, Luxemburg
33. Resch-Genger U, Bremser W, Pfeifer D, Spieles M, Hoffmann A, DeRose PC, Zwinkels JC, Gauthier FO, Ebert B, Taubert RD, Monte C, Voigt J, Hollandt J, Macdonald R (2012) State-of-the-art comparability of corrected emission spectra. I. Spectral correction with physical transfer standards and spectral fluorescence standards by expert laboratories. *Anal Chem* 84(9):3889–3898. <https://doi.org/10.1021/ac2034503>
34. Nakajima A (1976) Effects of isomeric solvents on vibronic band intensities in fluorescence-spectrum of pyrene. *J Mol Spectrosc* 61(3):467–469. [https://doi.org/10.1016/0022-2852\(76\)90336-2](https://doi.org/10.1016/0022-2852(76)90336-2)
35. Regev O, Zana R (1999) Aggregation behavior of Tyloxapol, a nonionic surfactant Oligomer, in aqueous solution. *J Colloid Interface Sci* 210(1):8–17. <https://doi.org/10.1006/jcis.1998.5776>
36. Mukerjee P, Mysels KJ (1970) Critical micelle concentrations of aqueous surfactant systems. National Bureau of Standards, Washington, DC
37. Lianos P, Viriot ML, Zana R (1984) Study of the solubilization of aromatic-hydrocarbons by aqueous micellar solutions. *J Phys Chem* 88(6):1098–1101. <https://doi.org/10.1021/J150650a014>
38. Zana R, In M, Lévy H, Duportail G (1997) Alkanediyol- $\alpha,\omega$ -bis(dimethylalkylammonium bromide). 7. Fluorescence probing studies of micelle micropolarity and microviscosity. *Langmuir* 13(21):5552–5557. <https://doi.org/10.1021/La970369a>
39. Jana B, Ghosh S, Chattopadhyay N (2013) Competitive binding of Nile red between lipids and beta-cyclodextrin. *J Photochem Photobiol B Biol* 126:1–10. <https://doi.org/10.1016/j.jphotobiol.2013.06.005>
40. Sarkar N, Das K, Nath DN, Bhattacharyya K (1994) Twisted charge transfer processes of Nile red in homogeneous solutions and in faujasite zeolite. *Langmuir* 10(1):326–329. <https://doi.org/10.1021/La00013a048>
41. Tajalli H, Gilani AG, Zakerhamidi MS, Tajalli P (2008) The photophysical properties of Nile red and Nile blue in ordered anisotropic media. *Dyes Pigments* 78(1):15–24. <https://doi.org/10.1016/j.dyepig.2007.10.002>
42. Felbeck T, Behnke T, Hoffmann K, Grabolle M, Lezhnina MM, Kynast UH, Resch-Genger U (2013) Nile-Red-nanoclay hybrids: red emissive optical probes for use in aqueous dispersion. *Langmuir* 29(36):11489–11497. <https://doi.org/10.1021/La402165q>
43. Chattopadhyay A, London E (1984) Fluorimetric determination of critical micelle concentration avoiding interference from

- detergent charge. *Anal Biochem* 139(2):408–412. [https://doi.org/10.1016/0003-2697\(84\)90026-5](https://doi.org/10.1016/0003-2697(84)90026-5)
44. Danov KD, Kralchevsky PA, Ananthapadmanabhan KP (2014) Micelle-monomer equilibria in solutions of ionic surfactants and in ionic-nonionic mixtures: a generalized phase separation model. *Adv Colloid Interface Sci* 206(0):17–45. <https://doi.org/10.1016/j.cis.2013.02.001>
45. Garcia-Mateos I, Mercedes Velazquez M, Rodriguez LJ (1990) Critical micelle concentration determination in binary mixtures of ionic surfactants by deconvolution of conductivity/concentration curves. *Langmuir* 6(6):1078–1083. <https://doi.org/10.1021/la00096a009>
46. Williams RJ, Phillips JN, Mysels KJ (1955) The critical micelle concentration of sodium lauryl sulphate at 25 °C. *Trans Faraday Soc* 51(0):728. <https://doi.org/10.1039/tf9555100728>
47. Phillips JN (1955) The energetics of micelle formation. *Trans Faraday Soc* 51(4):561–569. <https://doi.org/10.1039/tf9555100561>
48. Chiu YC, Wang SJ (1990) The micellar dissociation concentration of impure sodium dodecyl-sulfate systems in water. *Colloids Surf* 48(4):297–309. [https://doi.org/10.1016/0166-6622\(90\)80236-W](https://doi.org/10.1016/0166-6622(90)80236-W)
49. Chiu YC, Lin YW (1996) A general method for determining the micellar dissociation concentration of a surfactant using a differential refractometer. *Colloids Surf A* 106(1):23–31. [https://doi.org/10.1016/0927-7757\(95\)03341-6](https://doi.org/10.1016/0927-7757(95)03341-6)
50. Andreatta G, Bostrom N, Mullins OC (2005) High-Q ultrasonic determination of the critical nanoaggregate concentration of asphaltenes and the critical micelle concentration of standard surfactants. *Langmuir* 21(7):2728–2736. <https://doi.org/10.1021/la048640t>
51. Mehreteab A, Chen B (1995) Fluorescence technique for the determination of low critical micelle concentrations. *J Am Oil Chem Soc* 72(1):49–52. <https://doi.org/10.1007/Bf02635778>
52. Paillet S, Grassl B, Desbrieres J (2009) Rapid and quantitative determination of critical micelle concentration by automatic continuous mixing and static light scattering. *Anal Chim Acta* 636(2):236–241. <https://doi.org/10.1016/j.aca.2009.02.011>